atmosphere

MDPI

Article

Multi-Scale Urban Natural Ventilation Climate Guidance: A Case Study in the Shijiazhuang Metropolitan Area

Shuo Zhang [1], Xiaoyi Fang [1,*], Chen Cheng [1], Jing Chen [2], Fengxia Guo [3], Ying Yu [1] and Shanshan Yang [2]

[1] Chinese Academy of Meteorological Sciences, Beijing 100081, China; zhangshuo@cma.gov.cn (S.Z.); chengchen@cma.gov.cn (C.C.); yuying@cma.gov.cn (Y.Y.)
[2] Shijiazhuang Meteorological Bureau, Shijiazhuang 050004, China; cj640212@163.com (J.C.); sjzhjzxyss@163.com (S.Y.)
[3] Shijiazhuang Planning and Design Research Institute, Shijiazhuang 050051, China; 13315979281@163.com
* Correspondence: fangxy@cma.gov.cn

Abstract: The rapid development of urbanization has caused obstructed urban natural ventilation and the contribution rate of urbanization is relatively high. Therefore, there is an urgent need for urban development planning that should respect natural ventilation and local climate to reduce negative impacts. By optimizing the urban construction layout to reduce obstruction and leave a passageway for wind to blow in, the natural ventilation environment could be improved. This paper presents a promising approach for natural ventilation planning at both the city and community scales. Based on the assessment of wind environment, heat island intensity, and ventilation potential, the results revealed that winds blowing from the western and northern mountainous area of Shijiazhuang play a natural ventilation inlet role which can provide clean air. The SSHI and SHI were mainly distributed within the Second Ring Road, which has a large proportion of the low ventilation potential level. Thus, six first-class ventilation corridors and thirteen secondary corridors were recommended, which were set to be adapted to the dominant wind direction. Subsequently, an urban climate analysis map (UCAnMap) was developed considering climate sensitivity, and planning recommendations were provided for different climate zones. The relationship between architectural spatial structure and ventilation efficiency was analyzed; the results revealed that increasing the height of the buildings will decrease the proportion of comfortable wind zones, and the overall ventilation efficiency will weaken, so the average building height of a typical block should be controlled within 45 m, which matches ventilation performance requirements. The ventilation efficiency of the block has a certain negative correlation with the building density, and as the building density decreased by more than 10%, the proportion of the comfortable wind zones could increase by 4–5%.

Keywords: natural ventilation planning technology; ventilation corridors; UCAnMap; climate guidance

Citation: Zhang, S.; Fang, X.; Cheng, C.; Chen, J.; Guo, F.; Yu, Y.; Yang, S. Multi-Scale Urban Natural Ventilation Climate Guidance: A Case Study in the Shijiazhuang Metropolitan Area. *Atmosphere* **2024**, *15*, 676. https://doi.org/10.3390/atmos15060676

Academic Editors: Sen Chiao, Robert Pasken, Ricardo Sakai and Belay Demoz

Received: 7 April 2024
Revised: 9 May 2024
Accepted: 22 May 2024
Published: 31 May 2024

1. Introduction

The effectiveness of urban natural ventilation depends on the exchange and flow of air in an urban canopy, and it is related to the surrounding terrain, proportion of the impervious surface area, vegetation coverage type, and whether it is blocked by tall buildings. Numerous studies have shown that the surface energy balance is altered by the construction of physical urban infrastructure, driving detrimental impacts on urban climate such as increased temperatures and low-wind conditions [1]. Chen L et al. proposed that the existence of high-density and high-rise buildings has caused the narrowing of airflow channels or changes in direction when air passes through them, which easily forms a large scale of small wind zones on the leeward side of the buildings and significantly reduces the ventilation environment and climate comfort of a city. Peng Wang et al. (2021) showed that urbanization significantly increases the frequency of extreme heat in summer, and this trend is more prominent in densely populated and urbanized areas [2].

Due to the urbanization effect in Shijiazhuang, the annual average temperature significantly increased during 1981–2010, with a warming rate of 0.36 °C/10 a. Furthermore, from 1972 to 2012, the annual average wind speed decreased at a rate of −0.15 (m/s)/10a under an urbanization contribution rate of 86% [3]. Based on the air quality rankings of 74 cities that have already implemented the new city air quality standards published in 2017, Shijiazhuang ranked last, with an average annual proportion of excellent days of only 41.4% [4]. Therefore, there is an urgent need for planners and policy-makers to adopt Nature-Based Solutions with the lowest cost to reduce the negative impact on the local climate and make comfortable living conditions for high-quality urban living.

How can we leave a passageway for wind through optimizing an urban construction layout and allowing more natural wind to blow in? Chun-Ming Hsieh used the frontal area index (FAI) and the least cost path (LCP) methodology, identifying wind corridors based on the concept that wind moves along paths of low urban roughness [5]. Jeong min Son et al. used the KALM model to analyze the characteristics of local cold air, formed and maximized the use of it, and proposed wind corridor planning and management strategies in three Korean cities [6]. Shu Zheng et al. developed an empirical formula to determine an appropriate spatial domain for different combinations of building height, density, and arrangement, and they effectively predicted the influences and wind flow characteristics around a specific building in order to give suggestions on building layouts for a ventilation-friendly, livable urban environment [7]. However, there is a lack of a combination for urban natural ventilation research at both the city and community scales.

This paper, based on meteorological observation, numerical simulation, and remote sensing inversion methods, established a multi-scale natural ventilation planning technology which involves planning for fresh-air ventilation paths at the city scale, thereby giving suggestions on building layouts for ventilation performance requirements at the community scale and providing support for the effective connection of ventilation capacity between the whole city and typical blocks.

2. Study Area

Shijiazhuang is located in the southwestern part of Hebei Province, 270 km away from Beijing. The elevation of Shijiazhuang is shown in Figure 1. The elevation decreases from northwest to southeast. The western part of Shijiazhuang is located in the Taihang Mountains, with an elevation of about 1000 m, and the eastern part is located on the Hutuo River plain, with elevations of 30–100 m. Thus, the winds are blocked by the mountains, resulting in the weakening of the wind coming from the north and northwest. In addition, the southeast wind easily acts as a flux vortex. These wind-field conditions and characteristics in Shijiazhuang have resulted in its poor air circulation and difficulty in pollutant diffusion. The temporal and spatial distributions and daily changes in haze in Hebei Province were analyzed by Fu et al. [8]. The reason for the formation was discussed using hazy days in Shijiazhuang as a case study. The results revealed that the effect of the bell-mouth-shaped terrain plays a negative role in pollutant diffusion. The findings of Chen et al. also suggest that the terrain in the Taihang Mountains plays an important role in pollutant gathering [9].

In this paper, the central urban area and the four surrounding administrative districts of Shijiazhuang, namely Luquan, Zhengding, Gaocheng, and Luancheng, are taken as the study area, which is hereinafter collectively referred to as the metropolitan area. The study area is about 2638 km^2 (Figure 1). The metropolitan area received special attention in the 2017–2030 urban master plan revision of Shijiazhuang City. Its natural geographical characteristics and the distribution of meteorological stations used in this research are shown in Figure 1.

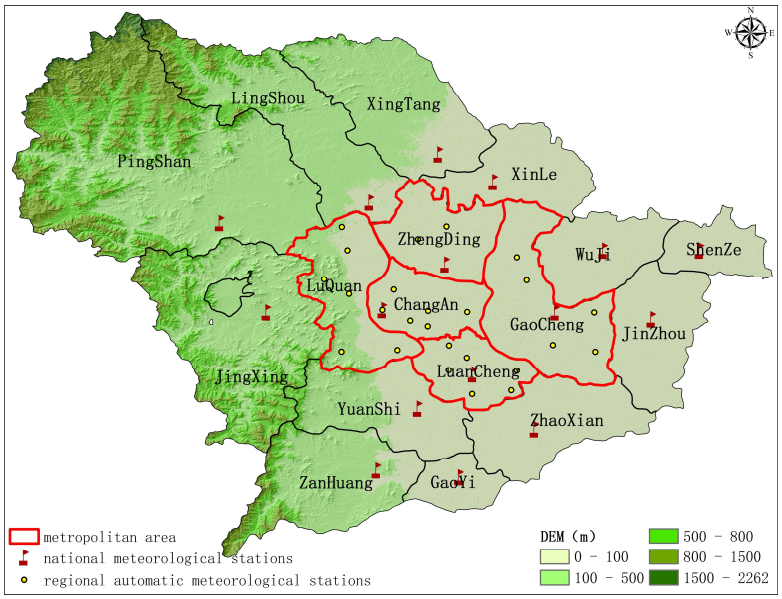

Figure 1. Geographical location and the distribution of the meteorological stations in Shijiazhuang City.

3. Data and Methods

The technical workflow of this research is shown in Figure 2.

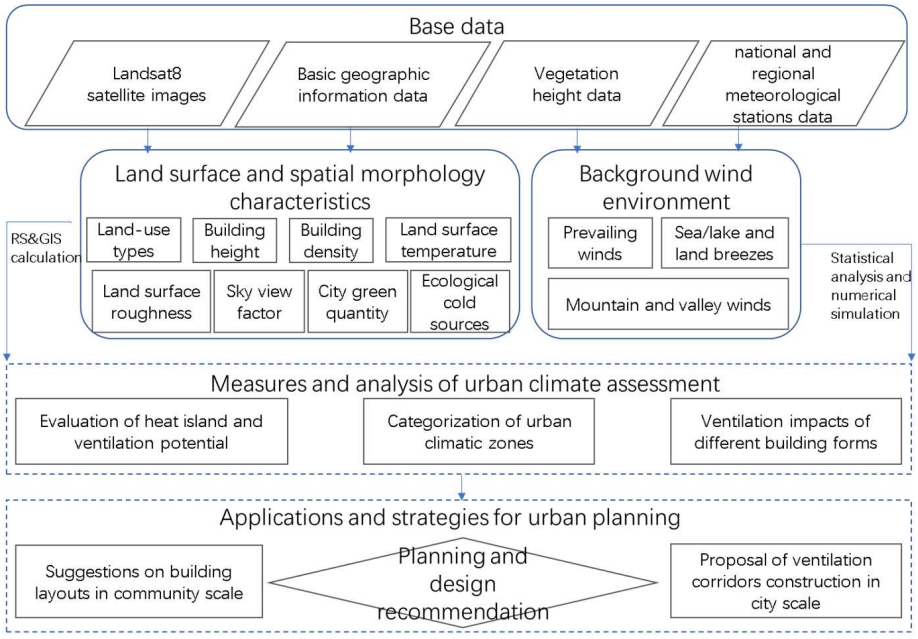

Figure 2. Research workflow diagram.

3.1. Data Acquisition

The meteorological data used in this paper were obtained from 16 national meteorological stations and 25 regional automatic meteorological stations of Shijiazhuang Meteorological Bureau, and they were subjected to quality control. Among them, the national meteorological stations provided climate compilation data from 1981 to 2010, which included the wind speed changes and the spatial distribution of wind directions, and they were used for the assessment of the prevailing wind environment in Shijiazhuang City. The regional automatic meteorological stations provided hourly data for the 10 min wind speed and wind direction between 2017 and 2018, which were used to identify the local

wind characteristics in the metropolitan area. Figure 1 shows the geographic location of these stations.

A satellite image of the clear sky with a resolution of 30 m in Shijiazhuang on 20 July 2018, from the Landsat8 operational land imager (OLI) sensor, was captured. It was mainly used to extract the land surface temperature, land use types, leaf area index, and green quantity. The thermal infrared sensor (TIRS) captured data with a resolution of 100 m, which were used to assess the heat loads. The data were obtained from the Geospatial Data Cloud (http://www.gscloud.cn/sources, accessed on 11 July 2018) and can be freely downloaded.

The basic geographical information data on a scale of 1:2000, which were acquired from the Shijiazhuang Planning and Design Research Institute, were used to calculate the ventilation potential assessment factors and to estimate the surface ventilation potential.

The global forest vegetation height data, which were inverted by the US Geoscience Laser Altimeter System (GLAS), were on a resolution of 1000 m. Meanwhile, for crop vegetation height, it was acquired from Shijiazhuang Agro-Meteorological Observing Station and obtained based on the physiological and phenological characteristics of crops in plain areas. Interpolation method was used to resample both the vegetation height of forest and crop to a resolution of 25 m, which were used to calculate surface roughness and ventilation potential in vegetation areas.

3.2. Methods

3.2.1. Assessment of Wind Environment

For winds with an excessive or slight velocity, the presence or absence of ventilation corridors has no obvious impact on the internal ventilation of the city. According to the Specifications for climatic feasibility demonstration—Urban ventilation corridor (QX/T 437-2018), the medium and small wind speed sections, which account for the largest proportion of wind frequencies, were regarded as soft and light breezes. The soft and light breezes can be used more efficiently in ventilation corridors to improve the actual ventilation effect [10]. According to the Beaufort wind scale, wind speeds of 0–0.2 $m \bullet s^{-1}$ represent calm wind, wind speeds of 0.2–1.5 $m \bullet s^{-1}$ represent light air, and wind speeds of 1.5–3.3 $m \bullet s^{-1}$ represent a light breeze. In this study, the statistics of the wind speed, direction, and frequency, and local characteristics of the soft and light breezes which affect the ventilation corridor were obtained, in order to conduct a background wind environment assessment and to grasp where the wind comes from and in what direction it probably will move.

3.2.2. Assessment of Thermal Environment

The Landsat 8 satellite image was used for surface temperature inversion and urban green quantity estimation. On this basis, heat island intensity assessment and ecological cold-source analysis can be carried out, and different local circulations will be generated according to the thermal differences between the heat islands and cold sources, accelerating the air flow inside the city.

The surface heat island intensity (SUHI) refers to the difference in the average land surface temperature between a certain location and the rural area, which is observed via remote sensing [11]. In this study, Landsat data were used for land surface temperature retrieval, and the SUHI was obtained. The heat island intensity was categorized into seven levels [12]: a strong cold island (SCI), sub-strong cold island (SSCI), weak cold island (WCI), no heat island (NHI), weak heat island (WHI), sub-strong heat island (SSHI), and strong heat island (SHI) (Table 1).

Studies have shown that in summer, urban surface temperatures follow the following pattern: bodies of water < forests < crops < lawns < bare lands < buildings [13]. Due to the temperature difference between the built-up area and water bodies or forest land, the flow of cold fresh air can be generated even under weak background wind conditions, which can effectively alleviate the urban heat island effect [14]. Therefore, bodies of water, forests, and crops, as well as urban green spaces with a high vegetation coverage, are defined as

natural cold sources. They are important zones that can produce cold, fresh air, and they play a fundamental role in natural ventilation planning and improve air circulation in the living environment.

Table 1. Levels and implications for different periods for SUHI.

Levels	Diurnal SUHI (°C)	Significance
1	SUHI < −7.0	SCI
2	−7.0 ≤ SUHI ≤ −5.0	SSCI
3	−5.0 < SUHI ≤ 3.0	WCI
4	−3.0 < SUHI ≤ 3.0	NHI
5	3.0 < SUHI ≤ 5.0	WHI
6	5.0 < SUHI ≤ 7.0	SSHI
7	>7.0	SHI

The green quantity is an important index that comprehensively reflects the vegetation leaf area index, vegetation coverage, and vegetation structure. It is considered to be an important parameter for measuring the ecological benefits and greening level of different spaces in cities and has significant effects for cooling, humidifying, and improving the urban microclimate [15]. It is calculated as follows:

$$S = 1/\ (1/30{,}000 + 0.000.2 \times 0.03NDVI)$$

$$NDVI = (b5 - b4)/\ (b5 + b4)$$

where S represents the urban green quantity (m^2), and b4 and b5 represent the reflectance of the 4th and 5th bands recorded by the Landsat8 OLI.

Eventually, taking both the land use type and green quantity into consideration, the ecological cold-source levels and their significance can be categorized [16] (Table 2).

Table 2. Green source levels and their significance.

Item	Levels			
	1	2	3	4
Land use types	Water body	Forest or Green Land	Forest or Green Land	Other
Green quantity (m^2)	-	Forest: ≥10,000 Green Land: ≥12,000	Forest: <10,000 Green Land: <12,000	Crops: ≥12,000 Sparse wood
Significance	SCS	SSCS	GCS	WCS

3.2.3. Estimating the Ventilation Potential

The ventilation potential refers to the air circulation capacity, which is determined by the surface vegetation, the coverage of the buildings, and the openness of the surroundings. Thus, the surface roughness length and sky-view factor (SVF) are essential indexes in the evaluation of the urban ventilation potential [16,17]. Since the ventilation potential is primarily related to the roughness of the underlying surfaces, the roughness in the urban built-up areas is mainly caused by buildings, while in the suburbs, it is mainly caused by vegetation. Therefore, the calculation of the roughness length is divided into two parts: that for urban areas and that for suburban areas.

1. For urban areas, buildings are the main factor that affects the momentum roughness of the air circulation in the atmospheric boundary layer [18]. A building morphological model was obtained using the 1:2000 topographic map and was used to extract two parameters: the building density and building height. Then, we obtained the surface roughness length in the urban areas with a resolution of 25 m.
2. For suburban areas, the surface roughness mainly depends on the vegetation type, leaf area index, and vegetation height. In this study, we used the polynomial regression

relationship between the leaf area index (LAI) and normalized vegetation index (NDVI), which was established by Wang et al. [19], as well as the morphological model parameters of the different vegetation types, which were determined by Jasinski et al. [20], and the method of calculating the vegetation canopy area index Λ, which was defined by Zeng et al. [21], was used to estimate the vegetation roughness in the suburban areas. Based on the survey data, there are two different vegetation types in the suburban areas: forest and crops. Therefore, we considered the differences in the vegetation height estimation method. The forest vegetation height was obtained from the global vegetation height data with a resolution of 1000 m, while the crop height was acquired from observations from the Shijiazhuang Agro-Meteorological Station [22]. In summary, the surface roughness length with a resolution of 25 m suburban areas in Shijiazhuang was obtained.

Open spaces are important areas for air circulation and urban ventilation and also serve as an important place for people's leisure and entertainment. Indeed, they are of great significance for the stability and optimization of the ecological environment [23]. The SVF is a description of the visible spatial characteristics and can quantitatively reflect the degree to which specific urban spaces are sealed off. In this study, the SVF was estimated using the raster calculation method based on a high-resolution digital elevation model (DEM) proposed by Zakšek et al. [24], and a 1:2000 topographic map's data were used to obtain a rafter model of the building elevation and the spatial distribution of the SVF with a resolution of 25 m in the metropolitan area.

Good natural ventilation requires a greater ventilation potential so that the wind passes through as easily as possible. According to Matzarakis [25], the primary indicator of a good air circulation capacity for a ventilation corridor is an aerodynamic roughness length of less than 0.5 m. Therefore, 0.5 m is regarded as the upper limit of the higher ventilation potential, and 1.0 m is regarded as the prescribed minimum. Oke [26] identified an inverse correlation between the SVF and urban heat island effect on the city block scale and found that the smaller the SVF is, the greater the probability and intensity of the urban heat island effect are. Chen et al. [17] studied the SVF in Hong Kong City and found that the upper limit of the effective range of the SVF in the relationship between the SVF and heat island intensity was 0.76. Therefore, the minimum value of the SVF for a relatively high ventilation potential is defined as 0.75. The ventilation potential was classified according to the principles presented in Table 3. The ventilation potential levels and their significance were used to identify the areas with a greater ventilation potential under the existing built-up area conditions.

Table 3. Ventilation potential levels and their significance.

Level	Significance	Roughness Length (Z0)	SVF (F)
1	Poor	$Z0 > 1.0$	—
2	General	$0.5 < Z0 \leq 1.0$	$F < 0.75$
3	Relatively high	$0.5 < Z0 \leq 1.0$	$F \geq 0.75$
4	High	$Z0 \leq 0.5$	$F < 0.75$
5	Very high	$Z0 \leq 0.5$	$F \geq 0.75$

3.2.4. Computational Fluid Dynamic Numerical Simulation

Optimizing the small-scale architectural spatial structure through reasonable air circulation guidance is necessary for the effective connection of ventilation capacity between the whole city and the local microclimate of the community scale. Computational fluid dynamic (CFD) numerical simulation is the main tool for studying the interaction and impact between the layout of the buildings and the local microclimate at the community scale [27–29]. Sketch Up physical design software was used for building a 3D model, and Wind perfect DX fluid dynamic software was used for simulation and calculation of wind environment around buildings [30,31]. In this study, we selected the surrounding area of Wanda Plaza as a typical block and used 1:2000 topographic map data to obtain the

building information and the distribution of the floors in this typical block. Based on the actual building height and shape boundaries, a three-dimensional model of this typical block was constructed. In addition, the model was imported into CFD software, and then all of the terrain and surface objects and their surroundings were gridded in order to finish the simulation parameter settings of the scale and azimuth.

Figure 3 shows the location and scope of this typical block, which extends from Huaibei Road in the north to Huai'an Road in the south and from Huaqing South Street in the west to Jianshe South Street in the east. The typical block is located in an urban construction area with various types of buildings, such as residential communities, commercial offices, and public services. The building height is between 3 and 102 m including multi-story buildings and high-rise buildings, and the building density is moderate at about 40–50%. Both the building height and building density are consistent with the characteristics of the average building parameters in the central urban area of Shijiazhuang. Thus, this typical block could serve as a good representation in the metropolitan area.

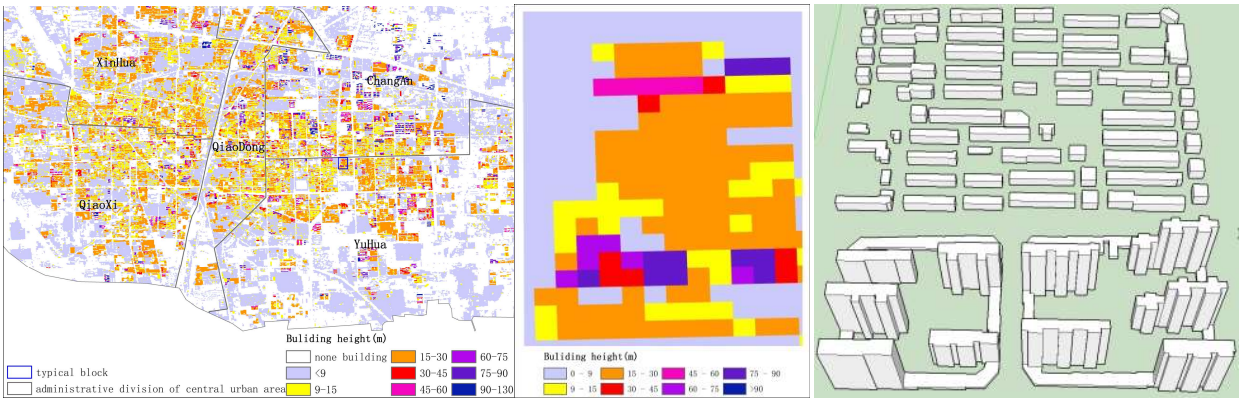

Figure 3. Location and 3D model of the typical block and its building height.

By adjusting the building height and density, the impact of the building form on the ventilation environment was studied. Using the control variate method, in which the building density remains unchanged and the building height takes different simulation schemes for the typical block, the wind field at different building heights was analyzed. Similarly, we adjusted the building density via the random and uniform removal of some buildings, with the building height remaining unchanged at the same time, and the wind environment of the typical block for different building densities was simulated. The six building-height simulation schemes and five building-density simulation schemes are described in Table 4. According to the comparison of the original wind fields and those under the simulation schemes with different building heights and building densities, the impact of the change in the building form on the wind environment was investigated [32,33].

Table 4. Simulation schemes for the typical block.

Simulation Scheme	Typical Block
Adjustment of building height	Decrease of 10 m per building Decrease of 5 m per building Increase of 5 m per building Increase 10 m per building Increase 15 m per building Increase 20 m per building
Adjustment of building density	Decrease of 5% Decrease of 10% Decrease of 15% Decrease of 20% Decrease of 25%

4. Results and Analysis

4.1. Analysis of Background Wind Environments

According to the national meteorological observation data from the Shijiazhuang stations, the south-southeast wind with a cumulative frequency of 12% was identified as the predominant wind direction throughout the year, followed by the north wind, with a cumulative frequency of 10%. In terms of the annual average wind speed of each wind direction, the south-southeast wind had the highest wind speed, followed by the west-northwest and west winds. The annual wind direction frequency statistics are shown in Figure 4. The results have shown that wind blowing from the western mountainous area with a high vegetation coverage was a significant source of clean air for the metropolitan area, including the west and northwest winds, making it the natural ventilation inlet of Shijiazhuang City. According to the statistics of the automatic meteorological stations, the dominant wind direction of the soft breeze was shown in Figure 5. The results indicate that as Luquan District is located along the mountainous area, due to the thermal difference between the mountainous area and the plain, the predominant wind direction of the soft breeze was mainly west and northwest. As Xinhua, Qiaodong, and Chang'an Districts are located in the northern part of the metropolitan area, the predominant wind direction of the soft breeze was mainly northeast and north. Qiaoxi and Yuhua Districts are located in the southern part of the metropolitan area and have a predominant wind direction of southeast and south. In Luancheng and Gaocheng District, the winds are predominantly south and southeast winds.

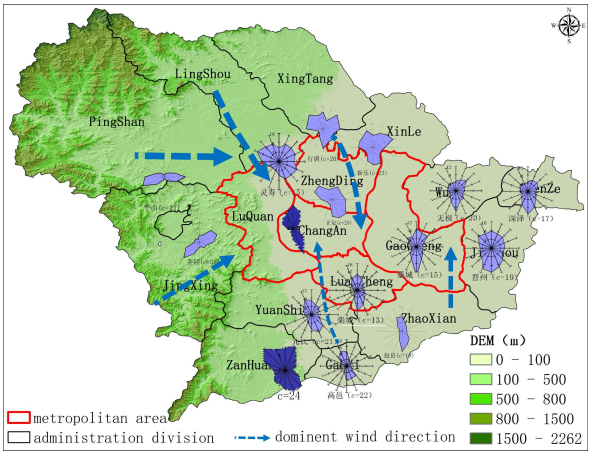

Figure 4. Spatial distribution of wind direction frequency in Shijiazhuang City.

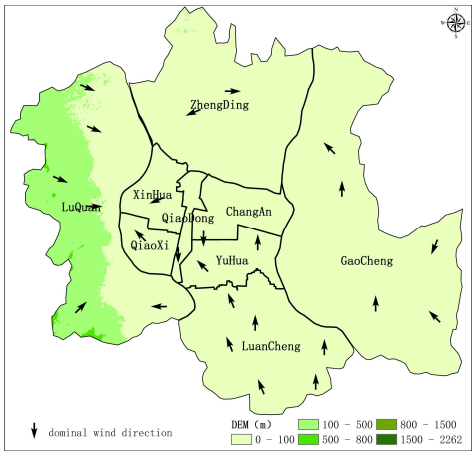

Figure 5. Dominant wind direction of the soft breeze in the metropolitan.

4.2. Analysis of Urban Heat Islands and Ecological Cold Sources

It was ascertained that the distribution of heat islands in the metropolitan area of Shijiazhuang was generally elliptical with an east–west long axis. The SSHI and SHI were mainly distributed within the Second Ring Road, and they were concentrated in the Xinhua, Qiaodong, and Chang'an Districts, as well as the commercial and industrial areas in Yuhua District (Figure 6a). Overlaying the land utilization situation (Figure 6b), it was observed that areas with a strong heat island effect were primarily characterized by impervious surfaces, with relatively less vegetation coverage. In addition, the heat island center extended significantly to the east and exhibited a contiguous trend from the central urban area to Gaocheng District.

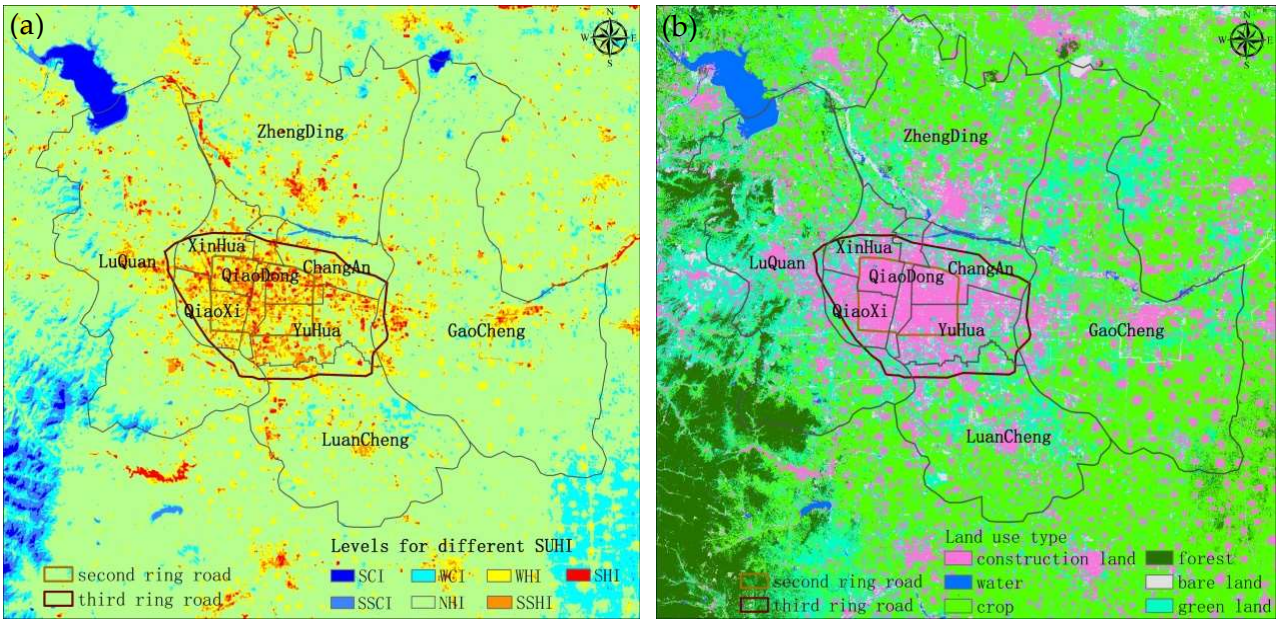

Figure 6. Spatial distributions of the heat islands (**a**) and land use types (**b**) in the metropolitan area.

As shown in Figure 7, the spatial distribution of the ecological cold sources exhibited the opposite pattern to the heat island, and the area within the scope of the heat island generally lacked cold sources. For example, the heat island area was concentrated within the Second Ring Road, and the ecological cold sources were scarce and dispersed in this area. The central area of the four surrounding administrative districts exhibited a significant heat island effect; however, it had a scarce distribution of ecological cold sources. The SCI was mainly located in the water body areas such as the Huangbizhuang Reservoir and Hutuo River, and it had a significant cold island effect. The SCI was mainly distributed in the mountainous area, specifically in the western part of Luquan District where the vegetation coverage was high. Indeed, the Hutuo River, which cut off the contiguous heat islands between Zhengding and the central urban area, played a significant role in relieving the heat island. The suburban green spaces and the large amount of farmland in the southeast plain were generally composed of a WCI and NHI, exhibiting a weak cold island effect, or at least the lack of a heat island.

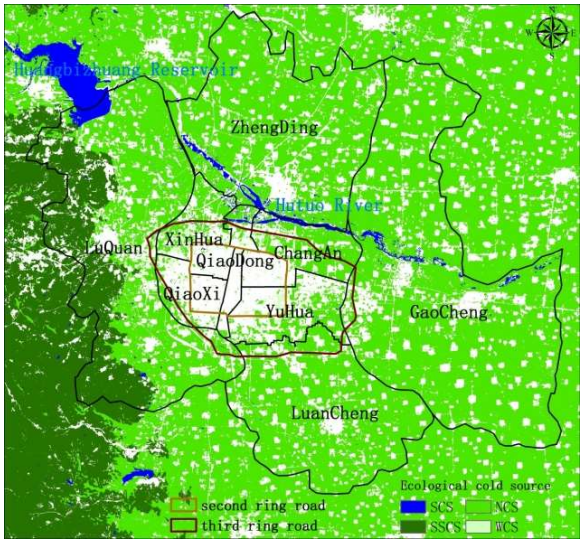

Figure 7. Spatial distribution of ecological cold sources in the metropolitan area.

4.3. Analysis of Urban Ventilation Potential

The spatial distribution of the roughness length (RL) in the metropolitan area was integrated using the RL in the urban and suburban areas (Figure 8). The results indicate that the RL of the urban area was relatively high, mostly exceeding 1 m, while it reached more than 3 m in some areas between the North Second Ring Road and the North Third Ring Road, as well as the western part of Chang'an District within the Second Ring Road. Due to the low building height and building density outside the Third Ring Road, the RL was generally less than 1 m, which was significantly lower than that within the Second Ring Road. The suburban area was mainly composed of forest, cropland, bare land, and water, with an RL ranging from 0 to 0.3 m, which is very similar to the results of Shinsuke K., who defined the values of water bodies, bare land, ice, flat grassland, and crops as 0.0002–0.25 m [34]. The RL value in Luquan District was relatively high, mostly between 0.2 m and 0.3 m, which was directly related to the high vegetation height in the mountainous areas [35].

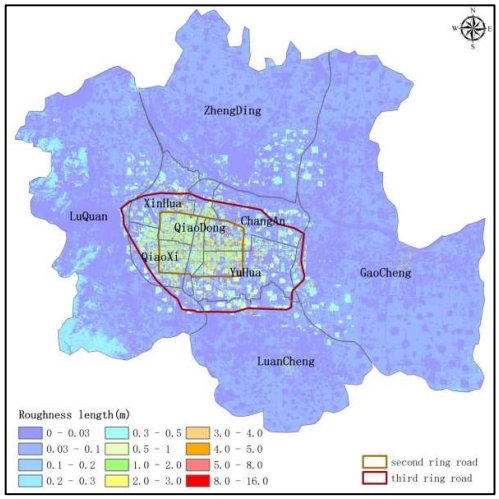

Figure 8. Spatial distribution of the roughness length in the metropolitan area.

The spatial distribution of the SVF in the metropolitan area with a resolution of 25 m was obtained from the 1:2000 topographic map data (Figure 9). The SVF in the region from the central part of Qiaodong District to the western part of Chang'an District, as well as the areas between the North Second Ring Road and the North Third Ring Road, was less

than 0.6 m. The values in the other urban built-up areas were generally between 0.6 m and 0.8 m. In some mountainous and piedmont areas, the RL value ranged from 0.7 m to 0.9 m, while in the surrounding plain areas the values were greater than 0.9 m.

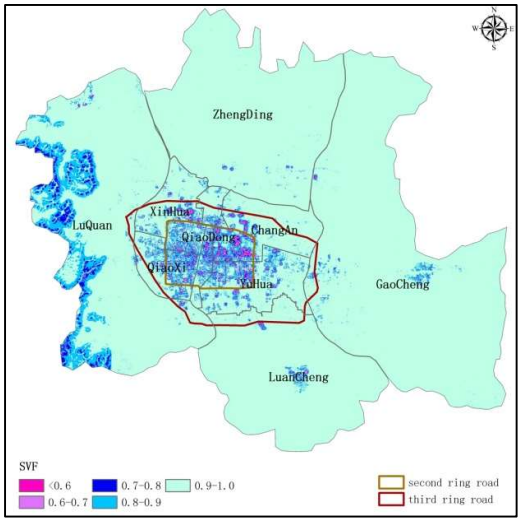

Figure 9. Spatial distribution of SVF in the metropolitan area.

The ventilation potential can be calculated by combining the sky-view factor and roughness length. Based on the above results, Figure 10 depicts the distribution of the ventilation potential classification with a resolution of 25 m for the metropolitan area. The results show that the overall surface ventilation potential within the Second Ring Road was poor, with a large proportion of a low ventilation potential level, while the areas with better ventilation capacities had smaller scales and lacked continuity. Except for the areas surrounding the Beijing–Guangzhou high-speed railway line, there was no available wide and continuous high-ventilation corridor in this area. In contrast, tiny river channels, parks and green spaces, wide streets, and low-rise buildings were identified between the Second Ring Road and Third Ring Road, had a high ventilation potential, and were scattered throughout the central urban area. Establishing connections between these high ventilation potential plots is conducive to creating a good ventilation environment. In addition, there were coherent and broad areas outside the Third Ring Road that had a high ventilation potential, and these areas had relatively good ventilation conditions.

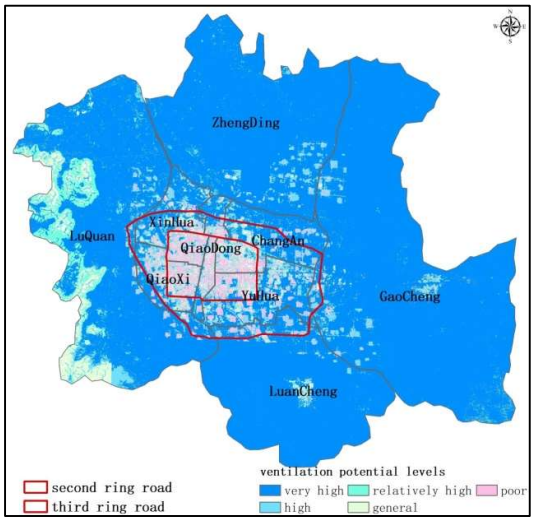

Figure 10. Spatial distribution of ventilation potential in the metropolitan area.

4.4. Analysis of Computational Fluid Dynamic Numerical Simulation

Based on the statistics of the annual average wind speed presented in Section 3.1, the initial meteorological conditions for the simulation were set. The west-northwest wind was selected as the input wind field, and the average wind speed was set to 1.7 m•s^{-1}. The atmospheric edge parameters were set as urban terrain with dense building clusters according to the load code for the design of building structures [36]. Due to the fact that the impact of the wind environment on human comfort is concentrated on the pedestrian-level wind velocity, which is about 1.5 m above the ground, the simulation results consisted of a 1.5 m height wind environment diagram and the corresponding wind speed values of the typical block.

According to Section 3.2.1, in this study, we calculated the number and percentage of the grids with three different wind speeds in the typical block, including calm wind, light air, and light breeze, in order to evaluate the quantitative impacts of the building height and building density adjustments on the wind environment in the typical block.

The evaluation of the impact of the building form on the wind environment in the typical block can be calculated using the ratio of the wind speed after the airflow passes through the building to the incoming flow speed (i.e., the average wind speed ratio, R). The impact of the building form on the wind environment can be calculated using the average wind speed ratio R, which is the ratio of the original wind speed to the wind speed after the airflow passes through the building. It serves as a ventilation performance parameter to evaluate the quality of the wind environment, reflecting the impact of the presence of buildings on the wind speed [9,10,34], and it can be calculated as follows:

$$R_i = \frac{V_i}{V_0}$$

Ri is the wind speed ratio at point i; V_i is the pedestrian-level wind velocity at point i, which is reflected in the average wind speed of the typical block; and V_0 is the undisturbed wind speed at the pedestrian level, which is usually taken as the initial wind speed.

Researchers have conducted on-site measurements of a large number of completed buildings and have conducted wind tunnel tests to establish models. By comparing different pedestrian-level wind comfort standards, they have summarized the relationship between wind speed probability and comfort at the pedestrian level (Table 5) [32,37,38]. Based on this, the comfort-limit wind speed was calculated, and the evaluation standard for the wind environment comfort was defined as a wind speed at the pedestrian level of 1 m•s^{-1} to 5 m•s^{-1}. The comfort wind zone ratio S, which is the proportion of the above wind speed range in the entire block, was also calculated. The larger the S value is, the greater the coverage of the comfort wind zone is, and this actually makes the wind environment better [38,39].

Table 5. Classification of comfort for pedestrian-level wind environment and the corresponding wind speed ranges.

Wind Speed Ranges	Comfort
1 m/s < V < 5 m/s	Comfort
5 m/s < V < 10 m/s	Discomfort, movement affected
10 m/s < V < 15 m/s	Significant discomfort, movement severely affected
15 m/s < V < 20 m/s	Insupportable
20 m/s < V	Dangerous

4.4.1. Impact of Building-Height Changes on Wind Environment

Figure 11 shows the spatial distribution of the wind fields in the typical block at a height of 1.5 m above ground under the different building-height simulation schemes, and Table 6 shows the corresponding changes in the different wind speed ranges. The results show that when the height of each building in the typical block was reduced, the

breeze zone on the leeward side of the buildings in the upwind area decreased, while the wind speed increased in the streets. The more the building height decreased, the more significant the increasing effect was. The proportion of the calm wind (wind speeds of <0.2 m•s^{-1}) decreased and the proportion of the light breeze (wind speeds of 1.5–3.3 m•s^{-1}) significantly increased. Under the simulation scheme of reducing the building height by 10 m per building, the proportion of the light breeze increased by about 3% compared to that for the original building height. This is consistent with the research findings of Ikegaya et al. [40], which show that the correlation coefficient between the wind speeds averaged over the entire region, the values in the front or side region were greater than 0.9, while in the area behind a building, the wind speeds were weakly correlated. The proportion of the calm wind in the typical block increased, and the proportion of the light air significantly decreased. Under the simulation scheme of increasing the building height by 20 m per building, the proportion of light air decreased by about 4% compared to that for the original building height, and the proportion of the light breeze increased slightly. This may be caused by the narrow pipe effect.

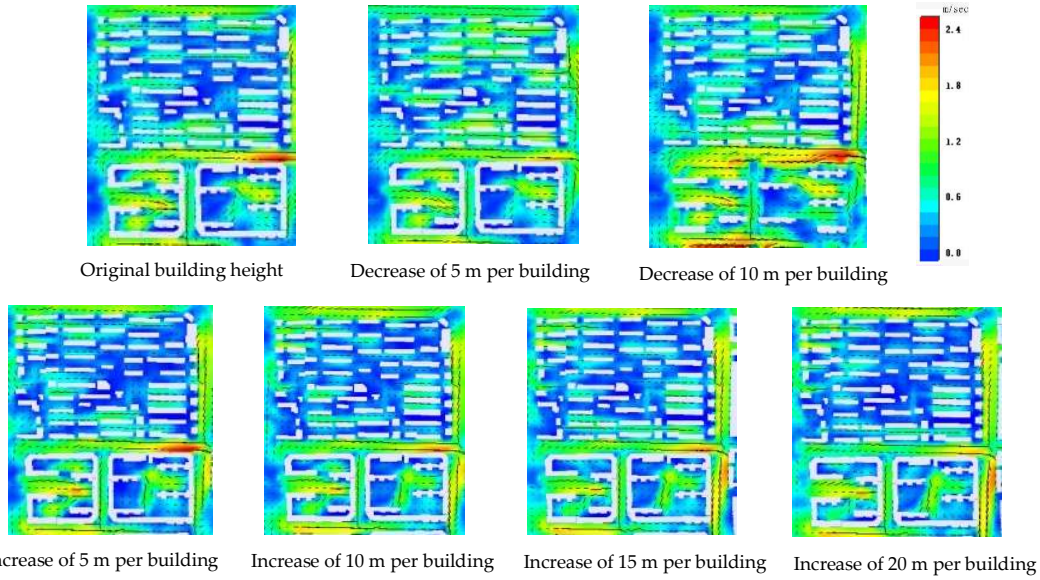

Figure 11. Spatial distribution of wind fields in the typical block at a height of 1.5 m above the ground under the different building-height simulation schemes.

Table 6. The number of grids and percentage in the different wind speed ranges under the seven building-height simulation schemes for the typical block.

	≤0.2 m/s		0.2–1.5 m/s		1.5–3.3 m/s	
	Number of Grids	**Percentage**	**Number of Grids**	**Percentage**	**Number of Grids**	**Percentage**
Decrease of 10 m per building	166	8.75%	1345	70.86%	387	20.39%
Decrease of 5 m per building	155	8.17%	1392	73.34%	351	18.49%
Original building height	187	9.85%	1384	72.92%	327	17.23%
Increase of 5 m per building	192	10.12%	1345	70.86%	361	19.02%
Increase of 10 m per building	198	10.43%	1347	70.97%	353	18.60%
Increase of 15 m per building	195	10.27%	1335	70.34%	368	19.39%
Increase of 20 m per building	220	11.59%	1302	68.60%	376	19.81%

The statistical results of the average wind speed ratio and the comfortable wind zone ratio at the pedestrian level in the typical block under the different building height

simulation schemes are presented in Table 7. It was found that the R value under the scheme with an increase of 20 m per building was less than 0.5, while under the schemes of increases of 5 m and 15 m per building, the R values were equal to 0.5. The R values for the schemes of a decrease of 10 m per building, a decrease of 5 m per building, and an increase of 10 m per building were greater than 0.5. Among them, the scheme of a decrease of 10 m per building had the highest R value. Based on the principle that the R value is no less than 0.5, we determined which construction form had the least impact on the wind speed reduction, and thus, we obtained a conclusion regarding the reasonable ranges of the building form parameters. The results also indicate that by reducing the height of each building, the proportion of the comfortable wind zones in the typical block will increase. Under the simulation scheme of a decrease of 5 m per building, the comfortable wind zone ratio will increase the most, by about 5% compared to that for the original building height. In contrast, if the height of each building is increased, the proportion of comfortable wind zones in the typical block will decrease. An increase of 20 m per building will lead to the largest decrease in comfortable wind zone ratio, by about 3% compared to that for the original building height. In summary, by reducing the building height, the average wind speed ratio and comfortable wind zone ratio of the typical block can be appropriately increased, resulting in an improvement in the ventilation environment.

Table 7. Statistics of wind environment indicators under the different building height simulation schemes for the typical block.

	Decrease of 10 m per Building	**Decrease of 5 m per Building**	**Original Building Height**	**Increase of 5 m per Building**	**Increase of 10 m per Building**	**Increase of 15 m per Building**	**Increase of 20 m per Building**
average wind speed ratio	0.57	0.52	0.53	0.50	0.51	0.50	0.49
comfortable wind zone ratio	41.04%	44.84%	40.09%	39.25%	38.99%	40.15%	37.67%

4.4.2. Impact of Changes in Building Density on Wind Environment

Similarly, the relationship between the average wind speed in the typical block and the building density was analyzed, and it a certain negative correlation was observed, the research results are consistent with Kubota, T. [41]. As the building density decreases, the small wind zones in the upwind direction are eliminated first, while those in the downwind direction are eliminated more slowly. If the number of buildings in the upwind direction is reduced, the wake effect of the building cluster will be weakened. If the number of buildings in the downwind direction is reduced, there will be no significant change in the average wind speed in the typical block. If the central building in the typical block was removed to set up an open space, the increase in the average wind speed would be very significant. Moreover, Table 8 has shown that if the building density is decreased slightly, the positive feedback effect on the ventilation performance of the typical block would not be sensitive. The more the building density decreases, the more obviously the proportion of the calm wind decreases and the proportion of the light breeze increases. For the scheme of a decrease in the building density of more than 20%, the proportion of the light-breeze areas will increases by about 3%–4% compared to that for the original building density situation.

There is a certain negative correlation between the average wind speed ratio of the typical block and its average building density, that is, reducing the building density can increase the average wind speed ratio. The more the building density decreases, the more obviously the average wind speed ratio increases. However, a slight decrease in the building density is not significant for the positive feedback effect of the average wind speed ratio. When the building density is decreased by 25%, the average wind speed ratio of the typical block exhibits a relatively high increasing trend. This indicates that the wind environment can only be improved by reducing the building density to a certain threshold.

Table 8. The number of grids and percentage in the different wind speed ranges under the six building density simulation schemes for the typical block.

	≤0.2 m/s		0.2–1.5 m/s		1.5–3.3 m/s	
	Number of Grids	**Percentage**	**Number of Grids**	**Percentage**	**Number of Grids**	**Percentage**
Original building density	187	9.85%	1384	72.92%	327	17.23%
Decrease of 5% in building density	187	9.75%	1399	72.98%	331	17.27%
Decrease of 10% in building density	188	9.67%	1396	71.77%	361	18.56%
Decrease of 15% in building density	194	9.88%	1390	70.81%	379	19.31%
Decrease of 20% in building density	215	9.71%	1392	70.32%	348	19.97%
Decrease of 25% in building density	186	8.60%	1482	70.52%	442	20.88%

According to the comfortable wind zone ratio at the pedestrian level in the typical block, as shown in Table 9, there is also a negative correlation between the comfortable wind zone ratio and the average building density. As the building density decreases, the proportion of the comfortable wind zones in the typical block gradually increases. When the building density is decreased by 5%, the difference in the proportion of the comfortable wind zone ratio is not obvious, indicating that if the building density decreases slightly, the positive feedback effect on the ventilation performance of the typical block would not be sensitive. When the building density is decreased by more than 10%, the proportion of the comfortable wind zones could increase by 4–5%, resulting in an improvement in the ventilation environment.

Table 9. Statistics of the wind environment indicators under the different building-density simulation schemes for the typical block.

	Original Building Density	**Decrease of 5% in Building Density**	**Decrease of 10% in Building Density**	**Decrease of 15% in Building Density**	**Decrease of 20% in Building Density**	**Decrease of 25% in Building Density**
Average wind speed ratio	0.53	0.54	0.54	0.54	0.54	0.56
Comfortable wind zone ratio	40.09%	42.04%	44.20%	44.41%	44.73%	45.09%

5. Application and Strategy

5.1. Construction of Wind Corridors Based on Climatopes

Based on the method of categorizing urban climatic zones, called climatopes, proposed by Yonghong Liu et al. [16], we unified the evaluation results of the thermal environment and ventilation potential to the same resolution, and then, we created an urban climate analysis map (UCAnMap) and produced a climatic analysis diagram for the metropolitan area of Shijiazhuang according to the climate sensitivity [42] (Figure 12). The red areas are mainly high-intensity development zones with a strong heat load, low ventilation potential, and extremely low vegetation coverage where the climate environment needs major improvement. The orange areas are mainly urban or rural construction areas with a relatively strong heat load and a poor ventilation potential. Unreasonable development of these areas will lead to the deterioration of the climatic environment. Thus, these areas considered to be the main target areas for future improvement and management in urban planning, and it is necessary to guard against an increase in the heat island and deterioration of the ventilation potential. The yellow areas are mainly the marginal regions of the orange areas, and they have a moderate heat load and relatively low ventilation potential. If the adjacent area of a red or orange area is large, the ecological isolation space should be taken into consideration. The light green areas are mainly low-heat-load zones with a relatively high ventilation potential. These areas have good vegetation coverage

and are always located in shallow mountainous areas, parks, or in the country side. The dark green areas are mainly the climate compensation areas with good vegetation coverage, such as suburban forests and farmland. These areas are considered to be ecological cold-source zones that produce cold fresh air, and attention should be paid to the protection of the vegetation coverage and ventilation potential. Based on the above analysis, the typical block is located in the red areas with strong heat load and low ventilation potential; therefore, carrying out research on its building form and layout optimization could provide a reference for improving local air conditions.

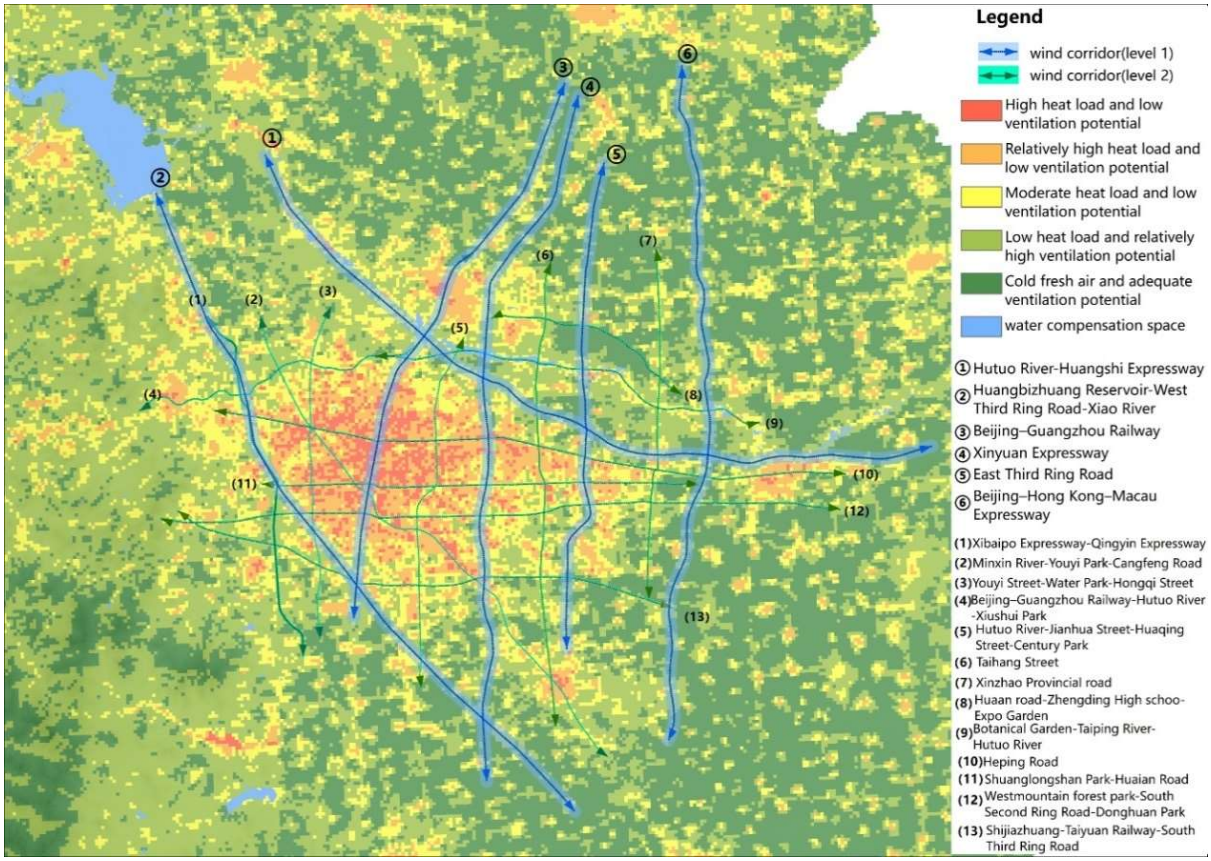

Figure 12. UCAnMap and natural ventilation corridor planning for the metropolitan area.

Based on the UCAnMap, a climate planning technique is proposed, and the natural ventilation corridors with effective climate resources and a high ventilation potential are applied in the metropolitan area of Shijiazhuang. The size and quantity of the air channels are related to the capacity and the required ventilation efficiency of the city. Therefore, if the edge length of the urban built-up area is L (km) and the wind speed is V (km•h^{-1}), the change in the daily air frequency is T, and T = 24 V/L. The proportion of the total width of the air channel (W) to the edge length of the city (L) is 1/T, so when W/L = 1T, L = WT, and W = L/T, then W = L1∗L2/24V [43]. The metropolitan area is about 26 km long in the east–west direction and 20 km long in the north–south direction, and the annual average wind speed is 1.7 m•s^{-1} (6.12 km•h^{-1}). According to the above equations, the change in the daily air frequency (T) in the east–west direction is 5.65 km, and the total width of the air channel (W) is 2.72 km. If each first-class ventilation corridor is about 1 km wide, two first-class corridors will be needed. Thus, the total remaining width of the secondary corridors is 0.72 km. Assuming that the average width of each secondary corridor is about 100 m, seven secondary corridors will be required. Regarding the north–south direction, T is 7.34 km and W is 4.6 km. Four first-class corridors with widths of 1 km and six secondary corridors with widths of 100 m are required. In summary, the total number of ventilation corridors in the metropolitan area is six first-class corridors and

thirteen secondary corridors [42] (Figure 12). Due to the fact that the wind source mainly comes from the western mountainous area, including the west and northwest wind, then the ventilation corridor is set to be northwest-southeast and east–west directions. In the coherent open spaces with the high ventilation potential of suburbs, first-class ventilation corridors could be formed, in order to bring fresh air from the edge of the city. Full use should be made of the rivers, such as the Hutuo River and its tributaries, as well as the forested green belts of the city's external transportation arteries including highways, national roads, and railways such as the Beijing–Guangzhou Railway and the Beijing–Hong Kong–Macao Expressway. It is important to take advantage of cold sources such as the Shijiazhuang Garden Expo, the Botanical Garden, and parks; large, open spaces such as Zhengding Station, Yunlong Bridge, and Zhengding Middle School; as well as main roads such as Heping Road, Huai'an Road, and the Second Ring Road that cross through the urban area, which are carriers for secondary ventilation corridors that export hot air from the urban area. In addition, the ventilation corridors should be evenly distributed in a network throughout the entire area as much as possible. By interconnecting the first-class corridors and extending the secondary corridors, a "blue net" may be formed, thereby promoting a healthy operation of urban air circulation.

5.2. Suggestions for the Buildings in the Block

In this paper, we present a general description of the impacts of the building height, building density, and other spatial layouts and forms on the wind environment of the typical block through six building-height simulation schemes and five building-density simulation schemes, with a total of twelve wind-field numerical simulations.

The ventilation efficiency of the typical block exhibits a certain negative correlation with the building height. When the height of each building in the typical block is decreased, the average wind speed ratio increases, the proportion of the calm-wind areas decreases, and the proportion of the light-breeze areas significantly increases. The more the building height is decreased, the more obvious the increasing effect is. In summary, the overall ventilation efficiency of the typical block will increase when the building height is decreased. When the height of each building in the typical block is increased, the average wind speed ratio decreases, the building height increases, and the average wind speed ratio decreases. The proportion of calm-wind areas increases, while the proportion of light-air areas significantly decreases, and the proportion of light-breeze areas slightly increases. In summary, the overall ventilation efficiency of the block will be weakened.

There is a certain negative correlation between the proportion of comfortable wind zones and the average building height. When the height of each building in the typical block is decreased, the proportion of the comfortable wind zones increases. When the height of each building is increased, the proportion of the comfortable wind zones in the typical block decreases. Based on the principle that the R value is no less than 0.5, we confirmed the reasonable control ranges of the corresponding building form parameters. According to the simulation results for the typical block, the R value is less than 0.5 under the simulation scheme with a decrease of 20 m per building, which is not consistent with the demands of the ventilation performance. Therefore, the threshold of the increase in the average building height in the typical block needs to be controlled within 20 m compared to the original building height, that is, only the building height controlled within 45 m can result in a smaller wind speed reduction effect.

The ventilation efficiency of the typical block has a certain negative correlation with the building density. Reducing the building density can increase the average wind speed ratio of the typical block. The more the building density decreases, the more obvious the increase in the average wind speed ratio is. When the building density is decreased by 5%, 10%, or 15%, the average wind speed ratio of these adjustment schemes does not exhibit a significant difference compared to that for the original building density. When the building density is decreased by 25%, the average wind speed ratio exhibits an increasing trend. As the building density decreases, the proportions of the calm wind and light

air generally decrease, while the proportion of the light breeze gradually increases. The more the building density decreases, the more significantly the proportions of the calm and light air decrease and the proportion of the light breeze increases. In summary, by decreasing the building density, the average wind speed ratio and comfortable wind zone ratio of the typical block can be appropriately increased, resulting in an improvement in the ventilation environment. However, if the decrease in the building density is smaller, the positive feedback effect on the ventilation performance of the typical block would not be sensitive. The more the building density is decreased, the better the wind environment will be. According to the results of this study, it is necessary to reduce the building density by about 20%.

6. Discussion

In this study, only the impact of building height and building density on wind environment was utilized, and the simulation schemes were evaluated under a specific meteorological background, which have certain limitations. The wind environment of a city is usually influenced by the building spatial form of the surroundings and not only the average height and density, but also the heterogeneity, arrangement patterns, as well as orientation [44]. Even if the average building height is the same, non-uniformity promotes the vertical mixing of air and increases ventilation efficiency. Even at the same building density, the effect on ventilation efficiency varies depending on the building arrangement pattern and orientation to the wind [45]. Therefore, it is also necessary to consider urban morphology and the arrangement patterns in optimizing ventilation to regulate urban environmental problems, and to compare the differences between the evaluation results, which would be effective for air circulation guidance and improving the local microclimate [46].

7. Conclusions

In this study, we established a natural ventilation planning technology based on the relationship between urban construction and the ventilation environment. We used indicators such as the SUHI, ecological cold source, and ventilation potential, and we also took into account urban climate sensitivity and effective climate resources, in order to analyze the spatial characteristics of the urban climate and develop an urban climate analysis map (UCAnMap). A "6+13" two-level ventilation corridor network, comprising six first-class ventilation corridors with widths of 1000 m and 13 secondary corridors with widths of 100 m, is proposed. Based on numerical simulation methods, we investigated the impacts of building height and building density on the wind environment and developed urban ventilation climate guidelines for the community scale, which was a kind of set of recommendations for the building form and layout control indicators. The results indicate that based on the principle that the average wind speed ratio is greater than or equal to 0.5, the appropriate ranges of the average building height and density can basically meet ventilation performance requirements. The optimum building height for the typical block was proposed, and these results can be used as a guide for controlling the building parameters, which is unique, highly original, and conducive to ventilation. However, mitigating the impacts of the building layout and establishing ventilation corridors are only two of the many considerations toward eco-city construction. Further research should be conducted on the relationship between the urban wind environment (UWE) and urban building energy (UBE), in order to reduce energy consumption from the perspective of UWE impact [22]; therefore, urban climates and living conditions may be greatly improved with science-based planning and constructions.

Author Contributions: Writing original draft, S.Z.; methodology, S.Z. and X.F.; Writing review & editing, X.F.; Formal analysis, C.C.; Supervision, J.C.; Resources, F.G.; Project administration, Y.Y.; Data curation, S.Y. All authors have read and agreed to the published version of the manuscript.

Funding: This research was funded by the National Key R&D Program of China (2022YFC3090600) and the Basic Research Fund of the Chinese Academy of Meteorological Sciences (No. 2023Z016).

Institutional Review Board Statement: Not applicable.

Informed Consent Statement: Not applicable.

Data Availability Statement: The raw data supporting the conclusions of this article will be made available by the authors on request. The data are not publicly available due to privacy.

Conflicts of Interest: The authors declare no conflict of interest.

References

1. Shi, J.; Liang, P.; Wan, Q.L.; He, J.H.; Zhou, W.D.; Cui, L.L. A review of the progress of research on urban climate. *J. Trop. Meteorol.* **2011**, *27*, 942–951.
2. Wang, P.; Luo, M.; Liao, W.; Xu, Y.; Wu, S.; Tong, X.; Tian, H.; Xu, F.; Han, Y. Urbanization contribution to human perceived temperature changes in major urban agglomerations of China. *Urban Clim.* **2021**, *38*, 100910. [CrossRef]
3. Bian, T.; Ren, G.Y.; Zhang, L.X. Significant urbanization effect on decline of near-surface wind speed at Shijiazhuang station. *Clim. Change Res.* **2018**, *14*, 21–30.
4. Cao, X.Y. Research on precise prevention and treatment of haze in Hebei province from the perspective of Beijing-Tianjin-Hebei coordinated development—A field research on prevention and treatment of haze in Shijiazhuang. *J. Shaanxi Inst. Econ. Manag.* **2018**, *26*, 20–24.
5. Hsieh, C.-M.; Huang, H.-C. Mitigating urban heat islands: A method to identify potential wind corridor for cooling and ventilation. *Comput. Environ. Urban Syst.* **2016**, *57*, 130–143. [CrossRef]
6. Son, J.M.; Eum, J.H.; Kim, S. Wind corridor planning and management strategies using cold air characteristics: The application in Korean cities. *Sustain. Cities Soc.* **2022**, *77*, 103512. [CrossRef]
7. Zheng, S.; Wang, Y.; Zhai, Z.; Xue, Y.; Duanmu, L. Characteristics of wind flow around a target building with different surrounding building layers predicted by CFD simulation. *J. Affect. Disord.* **2021**, *201*, 107962. [CrossRef]
8. Fu, G.Q.; Zhang, Y.X.; Gu, Y.L.; Zhang, Y.H. Change of haze day and its forming reason in Hebei province. *J. Meteorol. Environ.* **2014**, *30*, 51–56.
9. Chen, J.; Qian, W.M.; Han, J.C.; Wang, X.M.; Xu, M. Pollution characteristic under typical weather background in autumn over Shijiazhuang. *J. Meteorol. Environ.* **2015**, *31*, 42–50.
10. *QX/T 437-2018*; Specifications for Climatic Feasibility Demonstration—Urban Ventilation Corridor. China Meteorological Administration: Beijing, China, 2018.
11. Martin, P.; Baudouin, Y.; Gachon, P. An alternative method to characterize the surface urban heat island. *Int.-Natl. J. Biometeorol.* **2015**, *59*, 849–861. [CrossRef] [PubMed]
12. Jiang, X.D.; Xia, B.C. Spatial characteristics and dynamic simulations of urban heat environment of cities in Pearl River Delta. *Acta Ecol. Sin.* **2007**, *27*, 1461–1470.
13. Yue, W.Z.; Xu, L.H. Thermal Environment Effect of Urban Land Use Type and Pattern—A Case Study of Central Area of Shanghai City. *Sci. Geogr. Sin.* **2007**, *27*, 243–248.
14. Tong, H.; Liu, H.Z.; Li, Y.M.; Sang, J.H.; Hu, F. Actuality of summer urban heat island and the impact of urban planning "Wedge-Shaped Greenland" to reducing the intensity of urban heat island in Beijing. *J. Appl. Meteorol. Sci.* **2005**, *16*, 357–366.
15. Di, S.C.; Wu, W.Y.; Liu, H.L.; Yang, S.L.; Pan, X.Y. The co-relationship between urban greenness and heat island effect with RS technology: A case study within 5th ring road in Beijing. *J. Geo-Inf. Sci.* **2012**, *14*, 481–489.
16. Liu, Y.H.; Cheng, P.F.; Chen, P.; Zhang, S. Detection of wind corridors based on "Climatopes": A study in central Ji'nan. *Theor. Appl. Clim.* **2020**, *142*, 869–884. [CrossRef]
17. Chen, L.; Ng, E.; An, X.P.; Ren, C.; Lee, M.; Wang, U.; He, Z.J. Sky view factor analysis of street canyons and its implications for daytime intra-urban air temperature differentials in high-rise, high-density urban areas of Hong Kong: A GIS-based simulation approach. *Int. J. Climatol.* **2005**, *32*, 121–136. [CrossRef]
18. Zhang, Q.; Lv, S.H. The Determination of Roughness Length over City Surface. *Plateau Meteorol.* **2003**, *22*, 24–32.
19. Wang, X.X.; Sun, T.; Zhu, Q.J.; Liu, X.; Gao, F.F.; Hu, Y.M.; Chen, S.H. Assessment of different methods for estimating forest leaf area index from remote sensing data. *Acta Ecol. Sin.* **2014**, *34*, 4612–4619.
20. Jasinski, M.F.; Borak, J.; Crago, R. Bulk surface momentum parameters for satellite-derived vegetation fields. *Agric. For. Meteorol.* **2005**, *133*, 55–68. [CrossRef]
21. Zeng, X.B.; Shaikh, M.; Dai, Y.J.; Dickinson, R.E.; Myneni, R. Coupling of the common land model to the NCAR community climate model. *J. Clim.* **2001**, *15*, 1832–1854. [CrossRef]
22. Xue, J.; Hou, Z.F.; Liu, H.Y.; Yan, J.G.; Chen, Z. Study on the aerodynamic roughness of grassland shrub belt. *Agric. Res. Arid. Areas* **2016**, *34*, 253–256.
23. Luo, Q.Z.; Hang, W.; Yan, Y.C.; Li, X.H. Research on Calculating Sky view Factor with High Precision. *Remote Sens. Technol. Appl.* **2009**, *24*, 533–536.
24. Zakšek, K.; Oštir, K.; Kokalj, Ž. Sky-view factor as a relief visualization technique. *Remote Sens.* **2011**, *3*, 398–415. [CrossRef]
25. Matzarakis, A.; Mayer, H. Mapping of urban air paths for planning in Munchen. Planning applications of urban and building climatology. *Univ. Karlsruhe.* **1992**, *16*, 13–22.

26. Oke, T.R. Street design and urban canopy layer climate. *Energy Build.* **1988**, *11*, 103–113. [CrossRef]
27. Li, L.; Wu, D.; Zhang, L.J.; Yuan, L. Ventilation assessment on urban-block detailed planning based on numerical simulation. *Acta Sci. Circumstantiae* **2012**, *32*, 946–953.
28. Zhang, X.L.; Weerasuriya, A.U.; Lu, B.; Tse, K.T.; Liu, C.H.; Tamura, Y. Pedestrian-level wind environment near a super-tall building with unconventional configurations in a regular urban area. *Build. Simul.* **2020**, *13*, 439–456. [CrossRef]
29. Hagishima, A.; Tanimoto, J.; Nagayama, K.; Meno, S. Aerodynamic Parameters of Regular Arrays of Rectangular Blocks with Various Geometries. *Bound.-Layer Meteorol.* **2009**, *132*, 315–337. [CrossRef]
30. Zhuang, Z.; Yu, Y.B.; Ye, H.; Tan, H.W.; Xie, J.M. Review on CFD Simulation Technology of Wind Environment around Buildings. *Build. Sci.* **2014**, *30*, 108–114.
31. Shashua-Bar, L.; Tzamir, Y.; Hoffman, M.E. Thermal effects of building geometry and spacing on the urban canopy layer microclimate in a hot-humid climate in summer. *Int. J. Climatol. A J. R. Meteorol. Soc.* **2004**, *24*, 1729–1742. [CrossRef]
32. Gong, C.; Wang, X. Research on Wind Environment for Urban Residential District in Different Building Layouts. *Build. Sci.* **2014**, *30*, 6–12.
33. Qiao, Z.; Xu, X.; Wu, F.; Luo, W.; Wang, F.; Liu, L.; Sun, Z. Urban ventilation network model: A case study of the core zone of capital function in Beijing metropolitan area. *J. Clean. Prod.* **2017**, *168*, 526–535. [CrossRef]
34. Shinsuke, K.; Huang, H. Ventilation efficiency of void space surrounded by buildings with wind blowing over built-up urban area. *J. Wind. Eng. Ind. Aerodyn.* **2009**, *97*, 358–367.
35. Zhou, Y.L.; Sun, X.M.; Zhu, Z.L.; Zhang, R.H.; Tian, J.; Liu, Y.F.; Guan, D.X.; Yuan, G.F. Dynamic changes in surface roughness of several different underlying surfaces and their impact on flux mechanism model simulation. *Sci. China Ser. D Earth Sci.* **2006**, *36* (Suppl. I), 244–254.
36. *GB50009-2012*; Load Code for the Design of Building Structures. Ministry of Housing and Urban-Rural Development of the People's Republic of China: Beijing, China, 2012.
37. Gal, T.; Lindberg, F.; Unger, J. Comparing continuous sky view factor using 3D urban raster and vector databases: Comparison and application to urban climate. *Theor. Appl. Climatol.* **2009**, *95*, 111–123. [CrossRef]
38. Wang, Y.C. *Numerical Simulation Study of the Wind Environment for High Rise Residential District Based on Building Density and Plot Ratio*; Hebei University of Technology: Tianjin, China, 2015.
39. Blocken, B.; Janssen, W.D.; van Hooff, T. CFD simulation for pedestrian wind comfort and wind safety in urban areas: General decision framework and case study for the Eindhoven University campus. *Environ. Model. Softw.* **2012**, *30*, 15–34. [CrossRef]
40. Ikegaya, N.; Ikeda, Y.; Hagishima, A.; Razak, A.A.; Tanimoto, J. A prediction model for wind speed ratios at pedestrian level with simplified urban canopies. *Theor. Appl. Climatol.* **2017**, *127*, 655–665. [CrossRef]
41. Kubota, T.; Miura, M.; Tominaga, Y.; Mochida, A. Wind tunnel tests on the relationship between building density and pedestrian-level wind velocity: Development of guidelines for realizing acceptable wind environment in residential neighborhoods. *Build. Environ.* **2008**, *43*, 1699–1708. [CrossRef]
42. Zhang, S.; Fang, X.Y.; Chen, J.; Cheng, C.; Cheng, P.F.; Zhi, L.H.; Zhang, Q.; Yu, Y.; Du, W.P. Research on Urban Ventilation Corridor Planning Technology: A Case Study about Shijiazhuang Metropolitan Area. *Meteorol. Environ. Sci.* **2022**, *45*, 51–61.
43. Wang, S.; Li, M. Study on the Principle of Urban Open Space Eco-logical Planning. *Chin. Landsc. Archit.* **2001**, *17*, 32–36.
44. Jie, P.; Su, M.; Gao, N.; Ye, Y.; Kuang, X.; Chen, J.; Li, P.; Grunewald, J.; Xie, X.; Shi, X. Impact of urban wind environment on urban building energy: A review of mechanisms and modeling. *J. Affect. Disord.* **2023**, *245*, 110947. [CrossRef]
45. Janssen, W.D.; Blocken, B.; van Hooff, T. Pedestrian wind comfort around buildings: Comparison of wind comfort criteria based on whole-flow field data for a complex case study. *Build. Environ.* **2013**, *59*, 547–562. [CrossRef]
46. Hu, Y.D.; Liu, Z.H.; Tan, H.W. Multi-parameter Impact on Wind Environment of Residential District. *Build. Sci.* **2017**, *33*, 108–114.